JOURNAL OF BACTERIOLOGY, Oct. 1992, p. 6444–6454
0021-9193/92/206444-11$02.00/0

Vol. 174, No. 20

Rhodobacter sphaeroides rdxA, a Homolog of *Rhizobium meliloti fixG*, Encodes a Membrane Protein Which May Bind Cytoplasmic [4Fe-4S] Clusters

ELLEN L. NEIDLE AND SAMUEL KAPLAN*

Department of Microbiology and Molecular Genetics, University of Texas Health Science Center at Houston, P. O. Box 20708, Houston, Texas 77225

Received 22 May 1992/Accepted 3 August 1992

In the photosynthetic bacterium *Rhodobacter sphaeroides*, a chromosomal gene, *rdxA*, which encodes a 52-kDa protein, was found to be homologous to *fixG*, the first gene of a *Rhizobium meliloti* nitrogen fixation operon on the pSym plasmid (D. Kahn, M. David, O. Domergue, M.-L. Daveran, J. Ghai, P. R. Hirsch, and J. Batut, J. Bacteriol. 171:929–939, 1989). The deduced amino acid sequences of RdxA and FixG are 53% identical and 73% similar; sequence analyses suggested that each has five transmembrane helices and a central region resembling bacterial-type ferredoxins. Translational fusion proteins with an alkaline phosphatase reporter group were expressed in both *R. sphaeroides* and *Escherichia coli* and were used to assess the membrane topology of RdxA. Its ferredoxinlike sequence, which may bind two [4Fe-4S] centers, was found to be cytoplasmically located. Genetic disruptions showed that *rdxA* is not essential for nitrogen fixation in *R. sphaeroides*. Immediately downstream of *rdxA*, an open reading frame (ORFT2) that encoded a 48-kDa protein was found. This DNA sequence was not homologous to any region of the *R. meliloti fixG* operon. The N-terminal sequence of the ORFT2 gene product resembled amino acid sequences found in members of the GntR family of regulatory proteins (D. J. Haydon and J. R. Guest, FEMS Microbiol. Lett. 79:291–296, 1991). The *rdxA* gene was localized to the smaller of two *R. sphaeroides* chromosomes, upstream of and divergently transcribed from *hemT*, which encodes one of two 5-aminolevulinate synthase isozymes. The *rdxA* and *hemT* genes may share a transcriptional regulatory region. Southern hybridization analysis demonstrated the presence of an *rdxA* homolog on the *R. sphaeroides* large chromosome. The functions of this homolog, like those of *rdxA*, remain to be determined, but roles in oxidation-reduction processes are likely.

Rhodobacter sphaeroides is an α-purple nonsulfur eubacterium with diverse metabolic capabilities including the ability to grow aerobically, anaerobically, photosynthetically, and diazotrophically. Studies in our laboratory of 5-aminolevulinate (ALA) formation, the first and rate-limiting step in tetrapyrrole biosynthesis, led to the identification of an *R. sphaeroides* genetic homolog to *fixG*, a gene previously suggested to be involved in symbiotic nitrogen fixation by *Rhizobium meliloti* (35). The *R. sphaeroides* homolog, designated *rdxA* for redox, was found upstream of and divergently transcribed from the *hemT* gene, which encodes one of two ALA synthase isozymes (53, 68). The aim of this study was to determine the expression and function of *rdxA* in *R. sphaeroides*.

The specific role of *fixG* in *R. meliloti* has not yet been determined. The *fixGHI(S)* operon is located on the *R. meliloti* pSym plasmid; *fixG* is the first gene transcribed (35). Transposon Tn*5* insertions throughout the operon result in mutants that are unable to fix nitrogen. Hybridization studies with a probe containing part of *fixG* and the entire *fixH* and *fixI* genes have suggested strong conservation of these genes among rhizobia, although the region(s) of the probe responsible for hybridization was not localized among the three genes. FixI was predicted to be the catalytic subunit of a cation pump based on sequence similarities to ATPases (35). FixG, predicted to have five transmembrane regions, was found to have amino acid sequences that might coordinate iron-sulfur centers. FixG was predicted to be involved in an oxidation-reduction (redox) process, perhaps coupled to the FixI cation pump in a function specific for symbiotic nitrogen fixation (35).

As discussed below, the deduced amino acid sequence of RdxA would also suggest it to be a membrane protein involved in a redox process, although in free-living *R. sphaeroides* this process would not be specific for a symbiotic function. To determine the expression, localization, and topology of RdxA, translational fusions were made with an *Escherichia coli phoA* structural gene encoding alkaline phosphatase but lacking any signal sequences for protein export (44). Measurable PhoA activity results only from recombinant proteins in which an N-terminal *R. sphaeroides* peptide region can properly direct the C-terminal alkaline phosphatase moiety to the periplasm (70). In this study we constructed and examined the expression of RdxA::PhoA fusions in both *E. coli* and *R. sphaeroides*. In addition we studied the effects of an *rdxA* chromosomal disruption and the genomic environment of the wild-type locus to determine the function of this novel gene.

(Part of this work was presented at the 91st Annual Meeting of the American Society for Microbiology, Dallas, Texas, 1991.)

MATERIALS AND METHODS

Bacterial strains, plasmids, and growth conditions. Bacterial strains and plasmids are listed in Table 1. *R. sphaeroides* strains were grown with Sistrom's succinic acid minimal medium (41) supplemented as needed with antibiotics at the following concentrations: tetracycline, 1 μg/ml; streptomy-

* Corresponding author.

TABLE 1. Bacterial strains and plasmids

Strain or plasmid	Relevant characteristics	Reference or source
E. coli		
JM101	*supE thi* Δ(*lac-proAB*) F′ *traD36 proAB lacI*^{q}ZΔM15	47
S17-1	C600::RP-4 2-(Tc::Mu) (Km::Tn7) *thi pro hsdR hsdM*$^+$ *recA*	63
DH5α	*supE44* Δ*lacU169* (ϕ80 *lacZ* ΔM15) *hsdR17 recA1 endA1 gyrA96 thi-1 relA1*	3
R. sphaeroides		
2.4.1	Wild type	69
HemT1	2.4.1 derivative, *hemT*::Ω Sm^r Sp^r	53
RdxA1	2.4.1 derivative, *rdxA*::Ω Sm^r Sp^r	This study
Plasmids		
pUC19	Ap^r	71, 72
pBS	Ap^r, with T3 and T7 promoters	Stratagene
pSUP202	pBR325 derivative, Mob$^+$ Ap^r Cm^r Tc^r	63
pRK415	Tc^r	36
pHP45Ω	Source of Sp^r Sm^r cassette	56
pUI320	pUC19 derivative, *phoA* gene and restriction sites for making *phoA* translational fusions	70
pUI322	pRK415 derivative, polylinker upstream of *phoA*	70
pUI551	3.1-kb *hemT SalI* fragment in pUC19, DNA insert in the same orientation as *lac* promoter	68
pUI552	3.1-kb fragment of pUI551, opposite orientation	68
pUI1023	pUI320 derivative, *rdxA*::*phoA*, 395 *rdxA* codons	This study (Fig. 1)
pUI1024	DNA *rdxA*::*phoA* fragment of pUI1023 in pRK415	This study (Fig. 1)
pUI1026	pUI320 derivative, *rdxA*::*phoA*, 258 *rdxA* codons	This study (Fig. 1)
pUI1027	DNA *rdxA*::*phoA* fragment of pUI1026 in pRK415	This study (Fig. 1)
pUI1029	pSUP202 derivative, *rdxA*::Ω Sm^r Sp^r, 573-bp deletion in *rdxA*	This study (Fig. 1)
pUI1030	pUC19 derivative, *hemT*::Ω Sm^r Sp^r with 3.5 kb of DNA upstream of *hemT*, includes *rdxA* and ORFT2	This study (Fig. 1)
pUI1032	pBS derivative, 1.1-kb *SalI-BamHI rdxA* fragment	This study (Fig. 1)

cin, 50 μg/ml; and spectinomycin, 50 μg/ml. *R. sphaeroides* cultures were grown aerobically at 30°C on a rotary shaker or sparged with 30% O_2–69% N_2–1% CO_2. Photosynthetic cultures were grown photoheterotrophically in the light (10 W/m^2) in completely filled screw-cap tubes or sparged with 95% N_2–5% CO_2. A modified Sistrom's medium containing no source of reduced nitrogen was used for diazotrophic growth; K_2SO_4 was substituted for $(NH_4)_2SO_4$, Na_2MoO_4 was substituted for $(NH_4)_6Mo_7O_{24}$, and neither glutamate nor aspartate was added to the modified medium. Diazotrophically grown cells were sparged with 98% N_2–2% CO_2 and grown in light at an incident intensity of 10 W/m^2.

E. coli strains were grown at 37°C with Luria broth (43) supplemented as needed with antibiotics at the following concentrations: tetracycline, 10 μg/ml; streptomycin, 25 μg/ml; spectinomycin, 50 μg/ml; and ampicillin, 50 μg/ml. Isopropyl-β-D-thiogalactoside (40 μM) and 5-bromo-4-chloro-3-indolyl-β-D-galactoside (30 μg/ml) were used to monitor β-galactosidase activity in the construction of plasmids (71). Bacterial cell growth was monitored turbidometrically with a Klett-Summerson colorimeter with a no. 66 filter (1 Klett unit is equal to approximately 10^7 cells per ml).

DNA isolations, manipulations, and Southern hybridization techniques. Plasmids and DNA fragments were isolated, treated with modifying enzymes, and electrophoretically analyzed by standard techniques (43). Chromosomal DNA was isolated as previously described (19). Southern hybridizations (2 μg of DNA per lane) were carried out by using capillary transfer of the DNA to nitrocellulose or nylon membranes (43). Modifications for the transfer of high-molecular-weight DNA from pulsed-field electrophoresis gels were as described previously (65). Radioactive DNA or RNA probes with ^{32}P-labeled dCTP or CTP (Amersham Corp., Arlington Heights, Ill.) were made and utilized according to the manufacturers' instructions with nick translation systems (Bethesda Research Laboratories, Gaithersburg, Md.), random-primed DNA labeling kits (Boehringer Mannheim Biochemicals, Indianapolis, Ind.), or RNA transcription kits (Stratagene, La Jolla, Calif.). High-stringency conditions were used with hybridizations done at 42°C and final wash temperatures of 55°C. Radioactive signals were quantitated with a Betascope 603 blot analyzer (Betagen Corp., Waltham, Mass.).

Construction of a chromosomal gene disruption by omega cartridge interposon mutagenesis. The Ω Sm^r Sp^r DNA fragment of pHP45 (56) was used in the construction of a pSUP202 (63)-derived plasmid, pUI1029, carrying specifically modified *R. sphaeroides* DNA. Plasmid pUI1029 was introduced into *R. sphaeroides* wild-type strain 2.4.1, in which it cannot replicate, by previously described conjugation techniques (68). Transconjugants in which all or portions of pUI1029 had been chromosomally integrated by homologous recombination were selected for Sm^r Sp^r. These colonies were checked for Tc^s; of 200 Sm^r Sp^r *R. sphaeroides* isolates screened, 4 were found to be Tc^s. One of these was designated RdxA1 after Southern hybridization analysis.

Generation, deletion, and DNA sequence determination of subclones. DNA fragments of 0.1 to 2.5 kb were cloned into M13mp18 and M13mp19 vectors (71, 72). Nested deletion derivatives of the larger fragments were generated by using the Cyclone I Biosystem of International Biotechnologies, Inc. (New Haven, Conn.). The single-stranded ends of cloned DNA fragments were progressively digested by T4 DNA polymerase according to the manufacturer's instructions, and overlapping clones entirely covering both strands of the *rdxA* region were isolated. M13 bacteriophages were isolated, propagated, and used for the generation of single-stranded DNA sequencing templates (4). The DNA sequence was determined by the dideoxy-chain termination

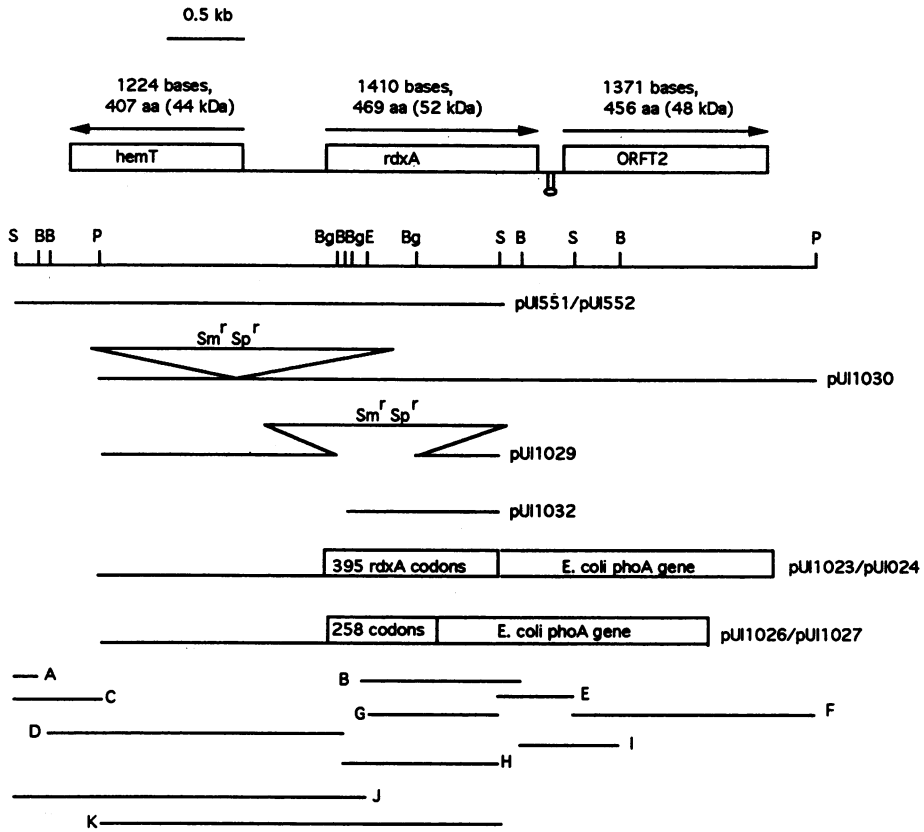

FIG. 1. Organization of the 5-kb *rdxA* chromosomal region of *R. sphaeroides*. The locations of three coding regions are shown above a map indicating the positions of sites recognized by restriction endonucleases *Sal*I (S), *Bam*HI (B), *Pst*I (P), *Bgl*II (Bg) and *Eco*RI (E). The sizes of each coding region and corresponding gene products and the direction of transcription are indicated for *rdxA*, *hemT*, and ORFT2. A potential stem-loop structure between *rdxA* and ORFT2 is depicted. Horizontal lines represent DNA fragments that were inserted into vectors, forming the plasmids indicated to the right. Insertion of the omega cartridge antibiotic resistance fragment Sm^r Sp^r (56) is marked. Letters A through K indicate fragments were used to determine the DNA sequence.

method (58) with commercial kits from U.S. Biochemical Corp. (Cleveland, Ohio) with the sequencing primer provided. α-^{35}S-dATP (>1,000 Ci/mmol) was purchased from the Amersham Corp. Sequencing reaction mixtures were electrophoretically separated on 8% polyacrylamide gels with 42% urea in Tris-borate-EDTA buffer, and then the gels were vacuum dried and autoradiographed.

DNA sequence analysis. Computer-assisted sequence analysis was done with PC/GENE software packages (IntelleGenetics, Inc., Mountainview, Calif.) and the University of Wisconsin Genetics Computer Group program (15). The GenEMBL and SwissProt data bases were screened for sequence similarities with algorithms based on that of Lipman and Pearson (42).

Alkaline phosphatase assays. *R. sphaeroides* and *E. coli* cells were fractionated, and alkaline phosphatase was measured in arbitrary units (8) as previously described (70). 5-Bromo-4-chloro-3-indolyl phosphate (XP; Sigma Chemical Co., St. Louis, Mo.) was used as a color indicator of alkaline phosphatase activity on bacterial agar plates at a concentration of 40 μg/ml.

Pulsed-field agarose gel electrophoresis. Genomic DNA was prepared and separated with a transverse alternating-field electrophoresis gel apparatus (Beckman Instruments, Inc., Fullerton, Calif.) as previously described (65).

Nucleotide sequence accession number. The 3,483-nucleotide sequence described in this report has been deposited with GenBank under accession number M94725.

RESULTS

Identification, isolation, and sequencing of *rdxA* DNA. Plasmids pUI551 and pUI552 (Fig. 1) each carry the *hemT* gene, which encodes one of two *R. sphaeroides* ALA synthase isozymes (68). Restriction endonucleases *Sal*I, *Eco*RI, *Bam*HI, and *Pst*I were used to generate DNA fragments (A, C, D, G, H, J, K; Fig. 1) for the DNA sequence determination of both strands of the 3,063-base *Sal*I insert of pUI551 and pUI552. Analysis revealed *rdxA* and indicated that additional chromosomal DNA was necessary to completely characterize this gene.

Chromosomal DNA was isolated from strain HemT1, an *R. sphaeroides* 2.4.1 derivative in which an omega cartridge Sm^r Sp^r marker disrupts the *hemT* gene (53). HemT1 DNA was completely digested with restriction endonuclease *Pst*I, ligated to pUC19, and used to transform *E. coli* JM101. Plasmid pUI1030 (Fig. 1) was selected for Ap^r Sm^r Sp^r. Southern hybridization analysis confirmed that the patterns of restriction endonuclease digestion of the newly isolated DNA matched those of wild-type chromosomal DNA in the region adjacent to *hemT* (data not shown). Restriction endonucleases *Eco*RI, *Bam*HI, *Sal*I, and *Pst*I generated DNA

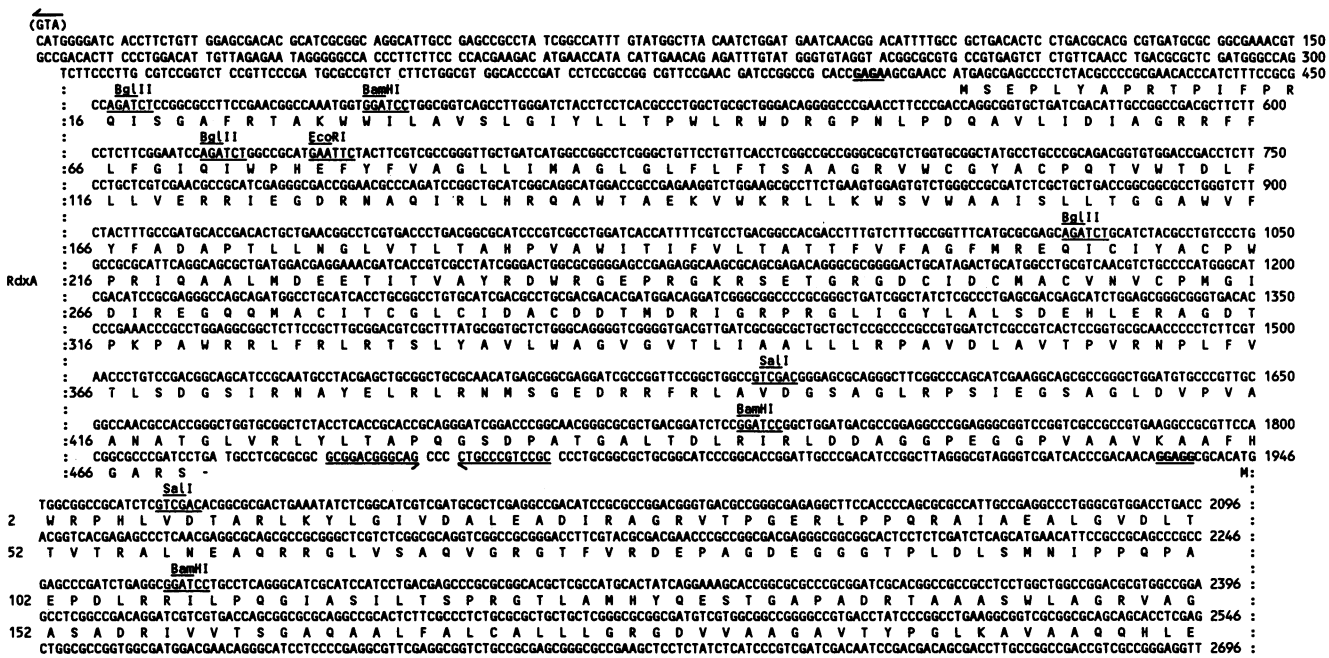

FIG. 2. DNA sequence of the *rdxA* region. The nucleotide sequence extends from immediately upstream of the *hemT* structural gene to the *Pst*I recognition site downstream of ORFT2 (Fig. 1). (GTA) indicates the oppositely transcribed *hemT* initiator codon. Deduced amino acid sequences are indicated immediately below the coding sequences of *rdxA* and ORFT2. Nucleotide and amino acid sequence positions are indicated to the right and left of adjacent bases and amino acid residues, respectively. Recognition sequences for several restriction endonucleases are underlined and indicated above the nucleotide sequence. Potential Shine-Dalgarno sequences (62) are indicated in boldface type and underlined. The arrows indicate an inverted repeat between *rdxA* and ORFT2.

fragments (B, E, F, I; Fig. 1) that were used to determine the complete nucleotide sequence of both strands of the DNA region shown in Fig. 1.

Open reading frame analysis and mol% G+C. In Fig. 2, 3,483 nucleotides of the DNA sequence from immediately upstream of the *hemT* structural gene to the *Pst*I recognition sequence of pUI1030 are presented. The *hemT* sequence (53) will be presented elsewhere. Computer analysis by two different methods (22, 39) suggested that two open reading frames transcribed in a direction opposite to that of *hemT*, designated *rdxA* and ORFT2, would be likely to encode proteins. The 1,410-base *rdxA* could encode a 469-amino-acid 52-kDa protein. The 1,371-base open reading frame, ORFT2, could encode a 456-amino-acid 48-kDa protein. Potential ATG-methionine initiation codons, preceded by possible ribosome-binding Shine-Dalgarno sequences (62), are indicated in Fig. 2.

The G+C content of the entire sequence shown in Fig. 2 was 69%, consistent with the high G+C content of *R. sphaeroides* DNA. The coding regions of *rdxA* and ORFT2 had G+C contents of 68 and 72%, respectively, whereas the sequence between *hemT* and *rdxA* was relatively A+T rich, with a G+C content of 59%. In the 127-nucleotide region separating *rdxA* and ORFT2, a region of dyad symmetry was found. This inverted repeat is shown in Fig. 2; the ΔG of a stem-loop formed by these 24 paired nucleotides was estimated to be −32 kcal (ca. −134 kJ).

Throughout *rdxA* and ORFT2, a relatively low second-position-codon G+C content and a relatively high third-position-codon G+C content were found, consistent with these being coding regions (5). The intervening DNA between the two genes had a uniform G+C distribution. The codon usages in *rdxA* and ORFT2 were compared with those of 15 previously studied *R. sphaeroides* genes. The codon usages in all genes were similar.

Sequence similarities to RdxA. Computer-assisted searches of the GenEMBL and Swiss-Prot data bases revealed significant homology between RdxA and FixG, encoded by a pSym-plasmid gene of *R. meliloti* (35). An alignment of the RdxA and FixG deduced amino acid sequences is shown in Fig. 3; 53% of the aligned residues are identical, and 73% of the aligned residues are similar or identical.

Similarities between a central region of RdxA and those of bacterial-type ferredoxins were also detected. The highly conserved pattern -Cys-X_1-X_2-Cys-X_3-X_4-Cys-X_5-X_6-X_7-Cys-(Pro) has been shown to be associated with the binding of a [4Fe-4S] cluster (2). Two such patterns of cysteine residues were found in RdxA at positions 251 and 275 (Fig. 3 and 4), although no proline was found in the pattern initiating with Cys-275. Homologies in these regions be-

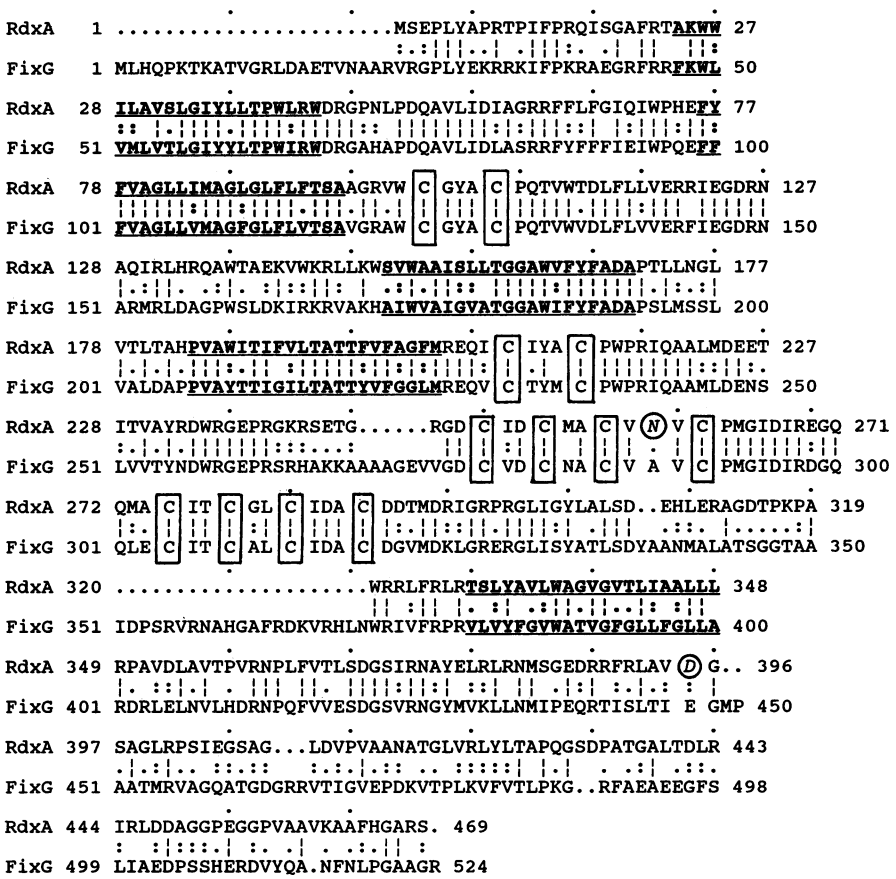

FIG. 3. Alignment of RdxA and FixG deduced amino acid sequences. Gaps (...) were introduced where necessary to optimize the alignment of similar (.:) and identical (¦) residues. Regions predicted to be transmembrane helices by the method of Eisenberg et al. (20) are indicated in boldface type and underlined. Cysteine residues that may be involved in iron-sulfur cluster binding are enclosed in boxes. RdxA residues at the junctions of RdxA::PhoA fusions are circled and shown in italics at positions 258 and 395.

tween RdxA and numerous ferredoxins and iron-sulfur proteins were detected. Alignments with some of these proteins are shown in Fig. 4.

With the Swiss-Prot data base (release 21.0), 11 of the 40 best protein sequence matches with RdxA were cytochrome *b* sequences from a variety of mammals (33). In pairwise comparisons of each cytochrome *b* sequence with RdxA, approximately 27% of aligned residues were identical over a 37-amino-acid stretch at the N-terminal portion of the proteins. An examination of the 40 best data bank sequence matches with either RdxA or FixG revealed similarity with numerous oxygenases and oxidoreductases in limited regions throughout the length of the amino acid sequences (Table 2).

Sequence similarities to ORFT2. Computer-assisted searches detected sequence similarities between the N-terminal region of ORFT2 and five proteins known or proposed to be regulatory proteins (Fig. 5) (10, 17, 23, 37, 64). Pairwise comparisons of the N-terminal sequences revealed approximately 20% identity between aligned amino acid residues. No homologies were detected between the C-terminal region of ORFT2 and other data base sequences.

Structure predictions based on deduced amino acid sequences. Analyses based on three different methods predicted RdxA to be a membrane protein. The method of Eisenberg et al. (20) predicted RdxA to have five membrane-spanning helices (underlined in Fig. 3). The method of Rao and Argos (57) predicted three transmembrane helices in RdxA at positions 76 through 103, 151 through 204, and 330 through 352. The method of Klein et al. (38) predicted three membrane-spanning segments at positions 78 through 94, 184 through 204, and 328 through 350.

The ORFT2 gene product was also examined. The method of Eisenberg et al. (20) detected no membrane associated helices. The method of Rao and Argos (57) predicted two transmembrane helices at amino acid positions 157 through 188 and 300 through 341. The method of Klein et al. (38) also predicted ORFT2 to encode an integral membrane protein. Two transmembrane segments were found at amino acid positions 157 through 176 and positions 320 through 336.

Secondary structure predictions by the method of Garnier et al. (27) suggested the N-terminal region of the ORFT2 protein to have an α-helix–β-turn–α-helix configuration common in regulatory proteins. A program in the PC/Gene software predicted the N-terminal region of the ORFT2 gene product to be a negative regulatory (repressor) protein. A helix-turn-helix region would also be suggested by alignment with a consensus sequence (Fig. 5) (18, 31).

Construction and analysis of *phoA* fusions. Fusion proteins were used to test the hypothesis that RdxA is a membrane protein. A transmembrane helix was predicted at approximately amino acid positions 329 through 348. RdxA::PhoA

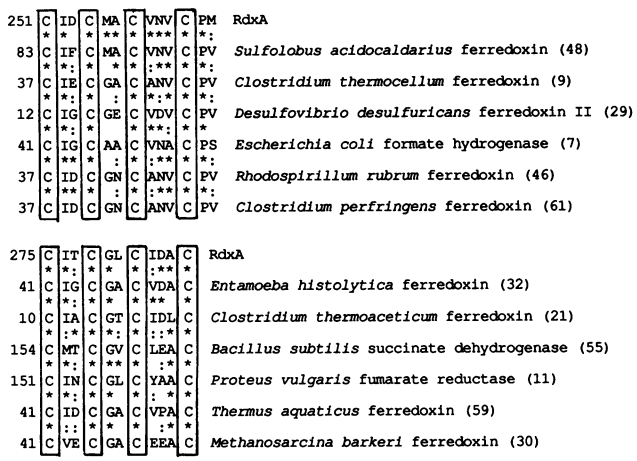

FIG. 4. Cysteine residues conserved in RdxA, ferredoxins, and other iron-sulfur proteins. Residues identical (*) and similar (:) to those of RdxA are indicated above the homologous protein sequence. Numbers indicate the positions of the adjacent residues in the protein sequences, and references for the iron-sulfur proteins are shown within parentheses. The spacing of the cysteines matches that found for bacterial ferredoxins that bind [4Fe-4S] clusters (2).

(alkaline phosphatase) hybrid proteins with fusion junctions before and after this helix at RdxA amino acid positions 258 and 395 were constructed. The 2,538-nucleotide *Pst*I-*Sal*I fragment of pUI552 was inserted into *phoA* fusion vector pUI320 to form pUI1023 (Fig. 1). The in-frame fusion between *rdxA* and *phoA* on pUI1023 was confirmed by DNA sequence determination. A fragment of pUI1023 including the recombinant *rdxA-phoA* DNA was transferred to pRK415 to form pUI1024 (Fig. 1). In pUI1023 and pUI1024, 395 codons of *rdxA* precede the *phoA* gene.

A 2,127-nucleotide *Pst*I-*Hin*cII fragment of pUI552 was joined to pUI320, forming an in-frame *rdxA-phoA* fusion (pUI1026, Fig. 1). The DNA sequence of the junction was confirmed. The recombinant *rdxA-phoA* DNA fragment was inserted into pRK415 to form pUI1027 (Fig. 1). Plasmids pUI1026 and pUI1027 each carry 258 *rdxA* codons joined to *phoA*.

Alkaline phosphatase was measured in strains 2.4.1 (pUI1024), 2.4.1(pUI1027), and 2.4.1(pUI322) grown aerobically and photoheterotrophically. Enzyme levels were also determined in *E. coli* DH5α(pUI1023), DH5α(pUI1026), and DH5α(pUI320). The *phoA* vectors pUI322 and pUI320 served as controls. Alkaline phosphatase activity was found only in strains 2.4.1(pUI1024), grown either aerobically or photosynthetically, and DH5α(pUI1023). Enzyme levels found in periplasmic, cytoplasmic, and membranous cell fractions are shown in Table 3; the results represent averages of at least three experimental repetitions. As expected (44), the majority of the pUI1024-encoded enzyme activity was found in the periplasm.

Strains 2.4.1(pUI1024), 2.4.1(pUI1027), 2.4.1(pUI322), DH5α(pUI1023), DH5α(pUI1026), and DH5α(pUI320) were grown with XP, which generates a blue product when cleaved by alkaline phosphatase. On XP-agar plates, 2.4.1 (pUI1024) and DH5α(pUI1023) led to a detectable blue color, whereas the other strains did not. The alkaline phosphatase activities in strains carrying pUI1023 or pUI1024 suggest that the region of the RdxA-PhoA junctions in the proteins encoded by these plasmids, at RdxA amino acid 395, is periplasmically located. In contrast, the region of the RdxA-PhoA junctions of the proteins encoded by pUI1026 and pUI1027, at RdxA amino acid 258, would appear to be cytoplasmically located. A topological model of RdxA based on these results and the prediction of membrane-spanning regions by the method of Eisenberg et al. (20) is shown in Fig. 6.

Construction and characterization of mutant strain RdxA1. At the 5′ region of *rdxA*, a 573-nucleotide deletion between *Bgl*II restriction endonuclease recognition sites (Fig. 2, positions 453 and 1026) was made, and the Ω Sm^r Sp^r cartridge (56) was inserted at this site. This disrupted *rdxA* gene carried on plasmid pSUP202-derived pUI1029 (Fig. 1) was introduced into wild-type strain 2.4.1. A mutant strain, RdxA1, in which the specifically disrupted *rdxA* replaced the chromosomal wild-type gene, was isolated. The chromosomal configuration of the *rdxA* locus of RdxA1 was confirmed by Southern hybridization analysis (data not shown).

Growth rates of RdxA1 under various physiological conditions were determined (Table 4). To ensure that no reduced nitrogen source was present in the medium utilized for diazotrophic growth, cells were inoculated and sparged with argon rather than nitrogen gas. In the absence of N_2 gas, no

TABLE 2. Oxygenases and oxidoreductases similar to RdxA or FixG

Enzyme (Swiss-Prot data base identifier) (reference)	RdxA or FixG amino acid at region start	% Identity of aligned residues	No. of amino acids in region compared
Cytochrome *c* oxidase (Sw:Cox3_Leita) (14)	FixG 361	39	36
Cytochrome P450 lauric acid hydroxylase	FixG 79	23	57
(Sw:Cp47_RABIT) (34)			
(Sw:Cp45_RABIT) (34)	FixG 105	29	31
NADH-ubiquinone oxidoreductase			
chain 4 (Sw:Nu4m_Ascsu) (54)	FixG 44	14	78
chain 1 (Sw:Nu1m_Drome) (26)	FixG 79	24	29
chain 5 (Sw:Nu5m_Mouse) (6)	FixG 482	60	10
(Sw:Nu5m_Rat) (25)	RdxA 362	37	19
Pyruvate-flavodoxin oxidoreductase (Sw:Nifj_Klepn) (1)	FixG 232	23	60
	RdxA 179	24	91
Cytochrome P450 steroid 11-β-hydroxylase	RdxA 137	50	14
(Sw:Cpn1_Human) (51)			
Luciferin 4-monooxygenase (Sw:Luci_Luccr) (45)	RdxA 358	32	22
Arachidonate-12-lipoxygenase (Sw:Lox2_Human) (24)	RdxA 367	32	34
Superoxide dismutase (Sw:Sodp_Pea) (60)	RdxA 362	22	65
Urate oxidase (Sw:Uric_Rabit) (52)	FixG 424	35	17

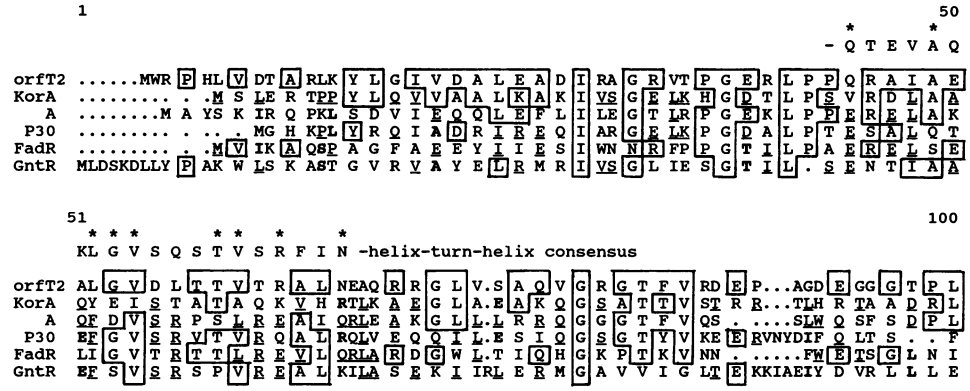

FIG. 5. Alignment of the N-terminal amino acid sequences of the ORFT2 gene product and bacterial regulators. The known or putative bacterial regulatory proteins are *Streptomyces lividans* KorA (37), *E. coli* A (GenA) (64), P30 (10), and FadR (17), and *B. subtilis* GntR (23). Residues identical to those encoded by ORFT2 are enclosed in boxes; identical aligned residues in two or more of the regulator sequences are underlined or indicated in boldface type. A consensus helix-turn-helix sequence (18, 31) is shown above the ORFT2 sequence in a region with nine residues identical to those of the consensus (*).

growth occurred. Under the aerobic, photoheterotrophic, and diazotrophic conditions tested, RdxA1 grew at a rate comparable to that of wild-type strain 2.4.1.

Chromosomal localization of *rdxA*. The RdxA1 Ω Sm^r Sp^r cartridge introduced two recognition sequences for restriction endonuclease *Ase*I, allowing precise chromosomal localization of the disrupted locus. The locations of wild-type chromosomal *Ase*I recognition sites were determined previously (66). Pulsed-field agarose gel electrophoresis and Southern hybridization analysis with *rdxA*-specific probes allowed the localization of *rdxA* on a 340-kb *Ase*I-generated DNA fragment on the smaller of two *R. sphaeroides* chromosomes (data not shown). The *rdxA* gene was found to be 17 kb from a reference *Ase*I recognition site, and it was found to be transcribed in a counterclockwise direction as depicted in Fig. 7C.

Identification and localization of an *R. sphaeroides rdxA* homolog. A 1.1-kb DNA fragment within *rdxA* was inserted into the pBS vector, forming pUI1032 (Fig. 1). Radioisotopically labeled *rdxA* RNA probes were generated from pUI1032 and used in Southern hybridization analysis of genomic 2.4.1 wild-type DNA digested with restriction endonucleases *Ase*I, *Ase*I and *Dra*I, and *Sna*BI and *Dra*I. After pulsed-field agarose gel electrophoresis, Southern hybridization, and autoradiography, two distinct bands were detected in each genomic digest even under stringent conditions (Fig. 7B). The stronger signal corresponded to the *rdxA* gene located on chromosome II. The weaker signal corresponded to hybridization between the *rdxA* probe and a region of chromosome I. The region of hybridization could be localized to a 190-kb *Sna*BI-*Dra*I chromosomal fragment (Fig. 7C).

Southern hybridization analysis of strain 2.4.1 DNA digested with restriction endonuclease *Sal*I and the pUI1032-generated probe led to the identification of the 3.1-kb *rdxA*-containing DNA fragment as well as to a weaker signal corresponding to a 4.2-kb DNA *Sal*I fragment (data not shown). Similar Southern hybridization analysis was done with the entire 3.1-kb *Sal*I fragment that carries both *rdxA* and *hemT* as a probe (Fig. 1). Signals to the 3.1- and 4.2-kb *Sal*I fragments were detected; in addition, a weak signal corresponding to the 7.2-kb *Sal*I DNA fragment carrying the *hemT* homolog *hemA* was detected (data not shown). Quantitation of the radioactive signals indicated that hybridization to the 4.2-kb *Sal*I fragment containing the *rdxA*-like sequence was at least 1.4-fold stronger than that to the 7.2-kb *Sal*I fragment containing *hemA*. The DNA sequences of the *hemT* and *hemA* genes have been determined; at the nucleotide level, the aligned sequences are 65% identical (53). These results suggest that the 4.2-kb *Sal*I DNA fragment identified by hybridization to *rdxA* carries a homolog of this gene and that the *rdxA* homolog resides on chromosome I (Fig. 7).

Southern hybridization analysis with probes from the ORFT2 region showed homologous ORFT2 signals, but under high-stringency conditions no additional chromosomal hybridization signals were revealed. A weak hybridization signal to the ORFT2 probe was detected, however, on the largest of the five *R. sphaeroides* endogenous plasmids (data not shown).

TABLE 3. Alkaline phosphatase activity of RdxA::PhoA fusions in *R. sphaeroides* 2.4.1 and *E. coli* DH5α

Strain[a]	Growth conditions	Alkaline phosphatase activity (U/min/mg of protein) in the following cell fraction:		
		Periplasm	Cytoplasm	Membrane
2.4.1(pUI1024)	Aerobic	6,583 ± 690	152 ± 84	570 ± 53
2.4.1(pUI1024)	Photosynthetic	2,883 ± 460	107 ± 21	545 ± 179
DH5α(pUI1023)	Aerobic	536 ± 49	74 ± 25	481 ± 87

[a] Strains 2.4.1(pUI1027), 2.4.1(pUI322), DH5α(pUI1026), and DH5α (pUI320) were also assayed, but specific alkaline phosphatase activity was less than 60 U/min/mg of protein in all fractions.

DISCUSSION

The *rdxA* gene encodes a membrane protein. In this report we describe the identification and isolation of a novel *R. sphaeroides* gene, *rdxA*, which is a homolog of *R. meliloti fixG*. Little is known about the expression or function of *fixG*, although it has been predicted to encode a membrane protein (35). In this study, alkaline phosphatase (PhoA) fusions were used to demonstrate that *rdxA* encodes an integral membrane protein in *R. sphaeroides*. The results of alkaline phosphatase measurements and computer-assisted

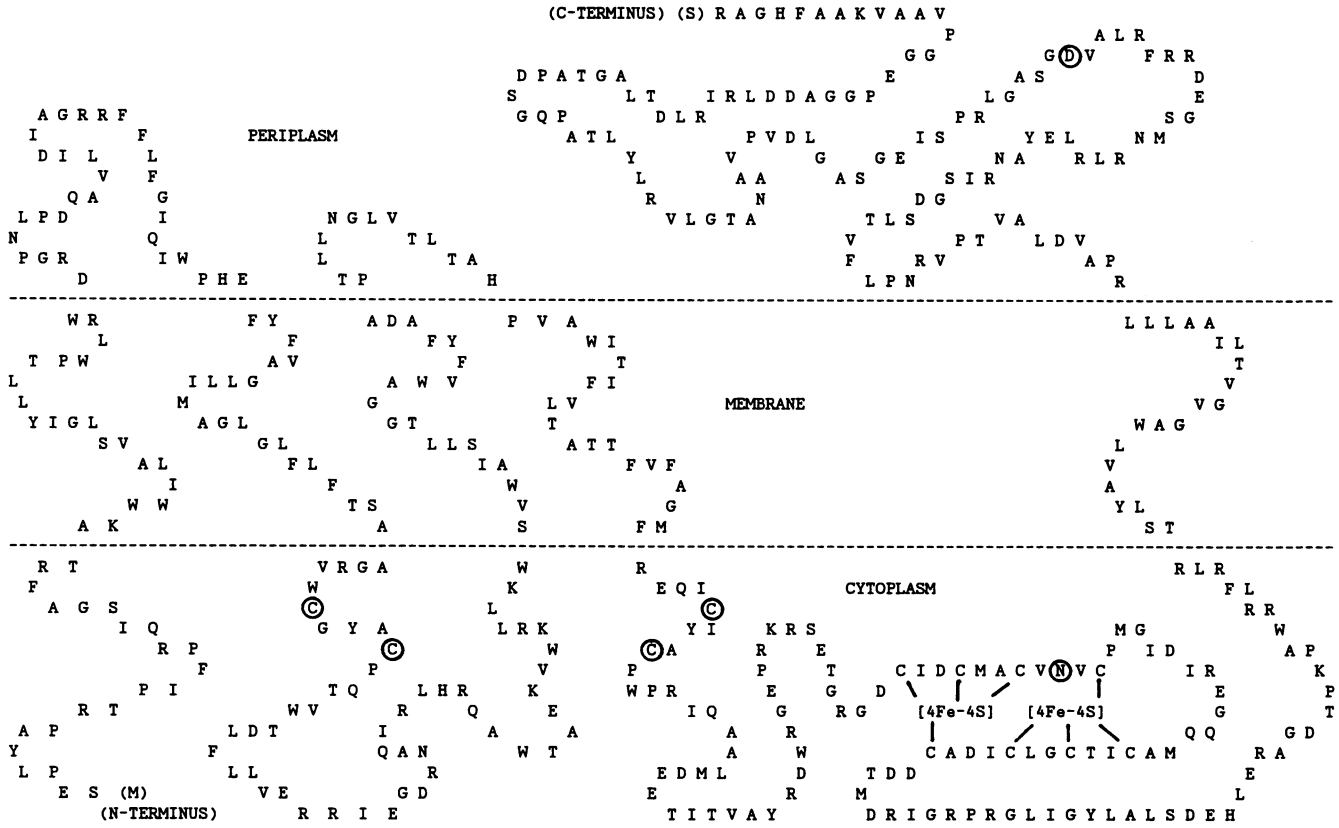

FIG. 6. Schematic representation of RdxA topology. Assignment of cellular localization is based on levels of alkaline phosphatase activity in strains carrying RdxA::PhoA fusions with junctions at residues N-258 and D-395, both encircled, and on predictions of transmembrane helices by the method of Eisenberg et al. (20). Potential iron-sulfur cluster binding to conserved cysteine residues is depicted. Additional cysteines that may be involved in iron-sulfur center coordination are encircled.

analyses of the RdxA sequence were used to assess membrane topology.

Periplasmic location was inferred for the site of the pUI1024-encoded hybrid protein junction, RdxA amino acid 395. The large, 121-amino-acid, C-terminal domain of RdxA would also be predicted normally to reside in the periplasm. In contrast, the site of the pUI1027-encoded hybrid protein junction, RdxA amino acid 258, in the region of conserved cysteines was inferred to be cytoplasmic. The entire 124-amino-acid domain between residues 204 and 328 of RdxA would also be predicted to be cytoplasmically located. Additional fusions are needed to confirm the topology of the N-terminal region of RdxA, but a model consistent with sequence analysis by the method of Eisenberg et al. (20) is presented in Fig. 6.

TABLE 4. Growth rates of RdxA1 and wild-type 2.4.1

Growth conditions	Generation time[a] (h) in strain:	
	2.4.1	RdxA1
Aerobic	2.8 ± 0.3	3.4 ± 0.8
Photoheterotrophic[b]	3.0 ± 0.4	3.2 ± 0.2
Diazotrophic[c]	7.5 ± 1.9	6.2 ± 0.8

[a] Averages of three or more independent determinations of doubling times.
[b] Incident light intensity of 10 W/m^2.
[c] No reduced nitrogen in medium. Cells were sparged with 98% N_2–2% CO_2 and grown in light with an incident intensity of 10 W/m^2.

Alkaline phosphatase activity in DH5α(pUI1023) but not DH5α(pUI1026) suggests that the *rdxA* gene can be expressed in *E. coli* with integration of the gene product in the same membrane orientation as that in *R. sphaeroides*. In plasmids pUI1023, pUI1024, pUI1026, and pUI1027, the *rdxA* initiation codon is separated from the *lac* promoter of the vector by approximately 1.4 kb of DNA. The lower enzyme levels of DH5α(pUI1023) than 2.4.1(pUI1024) may result from transcriptional dependence in *E. coli* on a distal vector promoter. It is also possible that in *E. coli* there is reduced stability or reduced membrane insertion of the hybrid protein. The observation of almost equal alkaline phosphatase activity in the periplasmic and membrane fractions of DH5α(pUI1023) could result from membrane localization of the fusion protein that is more stable than that in *R. sphaeroides*, or it could result from inefficient cell fractionation.

RdxA appears to be an iron-sulfur protein. The pattern of conserved cysteines in RdxA is that found for bacterial-type ferredoxins that bind two [4Fe-4S] clusters (2). This type of Fe-S cluster binding is found in many of the low-molecular-weight ferredoxins and in a variety of complex and multicomponent electron transfer proteins (2) (Fig. 4). The RdxA and FixG proteins may each bind two [4Fe-4S] centers, despite the aspartate residues rather than the usual prolines at positions 286 in RdxA and 315 in FixG.

Four additional cysteine residues, predicted to be cytoplasmically located, could be involved in iron-sulfur cluster

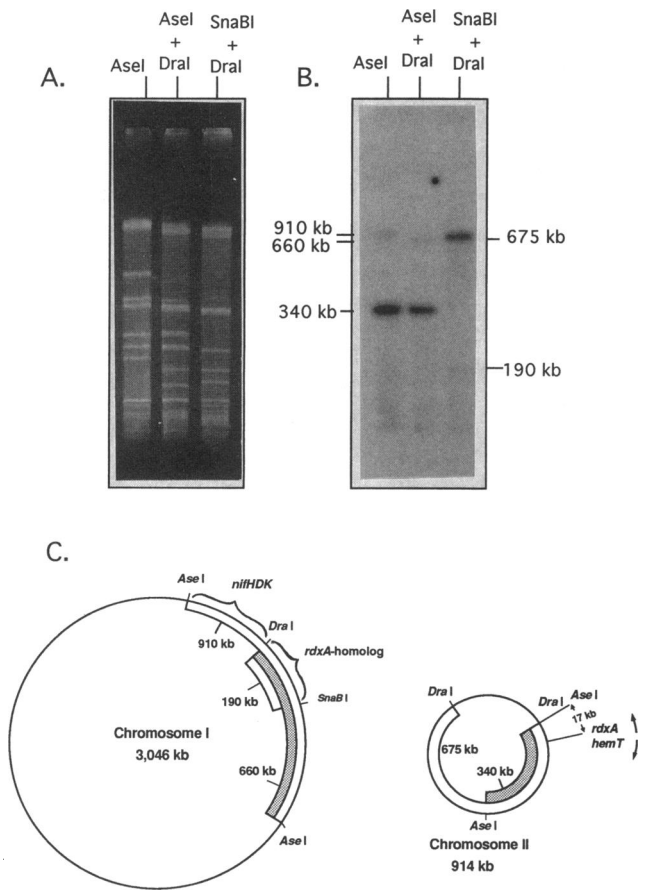

FIG. 7. Precise chromosomal localization of *rdxA* on chromosome II and regional localization of the *rdxA* homolog on chromosome I. (A) Ethidium bromide-stained pulsed-field electrophoresis gel of wild-type strain 2.4.1 genomic DNA digested with restriction endonucleases *Ase*I, *Dra*I, and *Sna*BI as labeled. (B) Autoradiogram of panel A after hybridization to an *rdxA* probe internal to the gene. Sizes of the DNA fragments corresponding to hybridization signals are indicated. (C) Depiction of the two *R. sphaeroides* chromosomes (not drawn to scale). The *rdxA* and *hemT* genes were located on chromosome II on a 340-kb *Ase*I fragment 17 kb from the reference *Ase*I site. Arrows indicate the direction of transcription for each gene. There are no *Sna*BI sites internal to the 675-kb *Dra*I fragment of chromosome II. Weak hybridization signals corresponded to an *rdxA* homolog on chromosome I, localized to a 190-kb *Sna*BI-*Dra*I fragment. The *nifHDK* genes are the only known *R. sphaeroides* genes involved in nitrogen fixation that have been localized. They were previously mapped to the 250-kb *Ase*I-*Dra*I fragment of chromosome I (65, 66), as shown.

binding. At RdxA positions 102 and 209, two cysteines match a portion of the pattern associated with iron-sulfur coordination, Cys-X-X-X-Cys-Pro (Fig. 3 and 6). These cysteines were conserved between RdxA and FixG.

Expression of *rdxA*. A 2.3-fold increase in alkaline phosphatase activity was found in strain 2.4.1(pUI1024) grown aerobically relative to that in the same strain grown photosynthetically. In *R. sphaeroides*, RdxA may be formed under both aerobic and photoheterotrophic conditions. Although expression of the native and heterologous *phoA* genes or proteins may differ, it does not appear that the RdxA membrane protein is specifically targeted to the specialized photosynthetic intracytoplasmic membrane.

The approximately 400 nucleotides that separate *rdxA* and *hemT* in *R. sphaeroides* are extremely rich in A+T nucleotides, perhaps indicating a regulatory region. We are currently exploring the role of this region in *hemT* regulation (53) and the possibility that this is a region of bent DNA (13). A consensus sequence upstream of *fixG* in *R. meliloti* suggests that its transcription is regulated by FixK, an Fnr-like regulator (12). No such consensus sequence was found upstream of *rdxA*, although this consensus sequence was found upstream of *pucBA* (40) and *hemA* (53) in *R. sphaeroides*.

The genetic organizations of *R. meliloti fixG* and *R. sphaeroides rdxA* differ. There appears to be translational coupling between the overlapping *fixG* and *fixH* genes (35). There are, however, 126 nucleotides separating *rdxA* and ORFT2, and in this region lies a potentially strong stem-loop ($\Delta G = -32$ kcal) that could act to stop transcription. No homology between ORFT2 and any other *fix* gene region was detected; the *fixGHI(S)* operon does not appear to correspond to an *rdxA* operon.

Possible roles of RdxA and its homolog in *R. sphaeroides*. The possibility that RdxA plays a role in an oxidation-reduction process is consistent with the similarities found between RdxA and ferredoxins (Fig. 4), oxidoreductases (Table 2), and cytochromes. This possibility is also consistent with the finding that the RdxA1 mutant is impaired in its ability to reduce tellurite to tellurium metal, particularly under aerobic conditions (49, 50). As discussed above, the RdxA levels under aerobic conditions may be higher than those under photoheterotrophic conditions. The RdxA1 phenotype may result from *rdxA* playing a direct role in tellurite reduction or an indirect role affecting the redox state of the cell.

rdxA was not found to be essential for nitrogen fixation in *R. sphaeroides*. In addition, high levels of RdxA::PhoA expression were found under aerobic conditions, although nitrogen fixation is strictly anaerobic in *R. sphaeroides*. A role for *rdxA* in nitrogen fixation, however, cannot be excluded. The presence of an *rdxA* homolog may mask phenotypic effects of the *rdxA* disruption. The presence of a homolog also emphasizes utilization of partial diploidy by *R. sphaeroides* (67). The hybridization intensity suggests that *rdxA* and its homolog are more similar than *hemA* and *hemT*, which at the nucleotide level are 65% identical (53).

The location of *rdxA* upstream of the divergently transcribed *hemT* suggests interdependent roles for the two genes. In *R. meliloti*, ALA formation plays a role in symbiotic nitrogen fixation; ALA^- mutants are unable to fix nitrogen. Bacterial ALA may be used in the heme moiety of the plant leghemoglobin apoprotein and/or it may affect nodule development (16). In addition, ALA is needed for the heme moiety of the *R. meliloti* FixLJ two-component regulatory system that responds to oxygen and controls the expression of nitrogen fixation genes (28). Similarly, possible joint roles in ALA formation and any redox process can be linked by the oxygen binding capacity of hemes and the electron transfer roles of cytochromes. Possible related functions of *rdxA* and *hemT* in *R. sphaeroides* need to be examined.

Identification and analysis of ORFT2. The N-terminal region of the ORFT2 gene product was found to resemble those of bacterial regulators (Fig. 5). KorA of *Streptomyces lividans* regulates plasmid transfer and replication (37). FadR is a transcriptional repressor of fatty acid degradation in *E. coli* (17). GntR represses the gluconate operon of *Bacillus subtilis* (23). The P30 and GenA proteins of *E. coli* may be

transcriptional regulators of genes encoding the α-ketoglutarate (64) and pyruvate dehydrogenase (10) complexes, respectively. The KorA, FadR, GntR, P30, and GenA regulators have been shown to belong to a family of bacterial regulators that also includes a histidine utilization regulator, HutC, of *Pseudomonas putida* and *Klebsiella aerogenes*, and PhnF, an *E. coli* protein of unknown function encoded in the *phn* locus, which determines alklyphosphonate uptake and carbon-phosphorus lyase activity (31).

All of these proteins have been found to have a DNA-binding helix-turn-helix motif in the N-terminal regions of their deduced amino acid sequences (Fig. 5) (31). With the exception of the 456-amino-acid ORFT2, the regulators are of similar sizes (236 to 248 amino acids). Even among the similarly sized proteins, however, the region of shared homology is limited to the N-terminal region depicted in Fig. 5 (31). Three computer programs used to analyze the ORFT2 sequence led to contradictory predictions of potential membrane-spanning helices. Further work is needed to determine a regulatory role for the ORFT2 gene product, to confirm the size and structure of the protein, and to determine the target region of its action.

ACKNOWLEDGMENTS

We thank K. Nereng and A. Suwanto for assistance with physical mapping techniques, S. C. Dryden for assistance with DNA sequence determination, and A. Varga for assistance with PhoA fusion techniques.

This work was supported by Public Health Service grant GM15590 to S.K. from the National Institutes of Health and by National Research Service Award GM13138 to E.N. from the National Institutes of Health.

REFERENCES

1. **Arnold, W., A. Rump, W. Klipp, U. B. Priefer, and A. Puhler.** 1988. Nucleotide sequence of a 24,206-base-pair DNA fragment carrying the entire nitrogen fixation gene cluster of *Klebsiella pneumoniae*. J. Mol. Biol. **203**:715–738.
2. **Beinert, H.** 1990. Recent developments in the field of iron-sulfur proteins. FASEB J. **4**:2483–2491.
3. **Bethesda Research Laboratories.** 1986. BRL pUC host: *E. coli* DH5α™ competent cells. Bethesda Res. Lab. Focus **8**:9–10.
4. **Bethesda Research Laboratories.** 1989. M13 cloning/dideoxy sequencing instruction manual. Bethesda Research Laboratories, Inc., Gaithersburg, Md.
5. **Bibb, M. J., P. R. Findlay, and M. W. Johnson.** 1984. The relationship between base composition and codon usage in bacterial genes and its use for the simple and reliable identification of protein-coding sequences. Gene **30**:157–166.
6. **Bibb, M. J., R. A. Van Etten, C. T. Wright, M. W. Walberg, and D. A. Clayton.** 1981. Sequence and gene organization of mouse mitochondrial DNA. Cell **26**:167–180.
7. **Bohm, R., M. Sauter, and A. Bock.** 1990. Nucleotide sequence and expression of an operon in *Escherichia coli* coding for formate hydrogenylase components. Mol. Microbiol. **4**:231–243.
8. **Brickman, E., and J. Beckwith.** 1975. Analysis of the regulation of *Escherichia coli* alkaline phosphatase synthesis using deletions and φ80 transducing phages. J. Mol. Biol. **96**:307–316.
9. **Bruschi, M., C. Cambillau, G. E. Bovier-Lapierre, J. J. Bonicel, and P. Forget.** 1986. Sequence determination and three-dimensional modelling of *Clostridium thermocellum* ferredoxin: structural considerations for its high thermal stability. Biochim. Biophys. Acta **873**:31–37.
10. **Buck, D., and J. R. Guest.** 1989. Overexpression and site-directed mutagenesis of the succinyl-coA synthetase of *Escherichia coli* and nucleotide sequence of a gene (g30) that is adjacent to the *suc* operon. Biochem. J. **260**:737–747.
11. **Cole, S. T.** 1987. Nucleotide sequence and comparative analysis of the *frd* operon encoding the fumarate reductase of *Proteus vulgaris*. Extensive sequence divergence of the membrane anchors and absence of an *frd*-linked *ampC* cephalosporinase gene. Eur. J. Biochem. **167**:481–488.
12. **Colonna-Romano, S., W. Arnold, A. Schluter, P. Boistard, A. Puhler, and U. B. Priefer.** 1990. An Fnr-like protein encoded in *Rhizobium leguminosarum* biovar *viciae* shows structural and functional homology to *Rhizobium meliloti* FixK. Mol. Gen. Genet. **223**:138–147.
13. **Crothers, D. M., T. E. Haran, and J. G. Nadeau.** 1990. Intrinsically bent DNA. J. Biol. Chem. **265**:7093–7096.
14. **De La Cruz, V. F., N. Neckelmann, and L. Simpson.** 1984. Sequence of six genes and several open reading frames in the kinetoplast maxicircle DNA of *Leishmania tarentolae*. J. Biol. Chem. **259**:15136–15147.
15. **Devereaux, J., P. Haeberli, and O. Smithies.** 1984. A comprehensive set of sequence analysis programs for the VAX. Nucleic Acids Res. **12**:387–395.
16. **Dickstein, R., D. C. Scheirer, W. H. Fowle, and F. M. Ausubel.** 1991. Nodules elicited by *Rhizobium meliloti* heme mutants are arrested at an early stage of development. Mol. Gen. Genet. **230**:423–432.
17. **DiRusso, C. C.** 1988. Nucleotide sequence of the *fadR* gene, a multifunctional regulator of fatty acid metabolism in *Escherichia coli*. Nucleic Acids Res. **16**:7995–8009.
18. **Dodd, I. B., and J. B. Egan.** 1987. Systematic method for the detection of potential λ Cro-like DNA-binding regions in proteins. J. Mol. Biol. **194**:557–564.
19. **Dryden, S. C., and S. Kaplan.** 1990. Localization and structural analysis of the ribosomal RNA operons of *Rhodobacter sphaeroides*. Nucleic Acids Res. **18**:7267–7277.
20. **Eisenberg, D., E. Schwarz, M. Komaromy, and R. Wall.** 1984. Analysis of membrane and surface protein sequences with the hydrophobic moment plot. J. Mol. Biol. **179**:125–142.
21. **Elliott, J. I., S.-S. Yang, L. G. Ljungdahl, J. Travis, and C. F. Reilly.** 1982. Complete amino acid sequence of the 4Fe-4S, thermostable, ferredoxin from *Clostridium thermoaceticus*. Biochemistry **21**:3294–3298.
22. **Fickett, J. W.** 1982. Recognition of protein coding regions in DNA sequences. Nucleic Acids Res. **10**:5303–5318.
23. **Fujita, Y., T. Fujita, Y. Miwa, J. Nihashi, and Y. Aratani.** 1986. Organization and transcription of the gluconate operon, *gnt*, of *Bacillus subtilis*. J. Biol. Chem. **261**:13744–13753.
24. **Funk, C. D., L. Furci, and G. A. Fitzgerald.** 1990. Molecular cloning, primary structure, and expression of the human platelet/erythroleukemia cell 12-lipoxygenase. Proc. Natl. Acad. Sci. USA **87**:5638–5642.
25. **Gadaleta, G., G. Pepe, G. De Candia, C. Quagliariello, E. Sbisa, and C. Saccone.** 1989. The complete nucleotide sequence of the *Rattus norvegicus* mitochondrial genome: cryptic signals revealed by comparative analysis between vertebrates. J. Mol. Evol. **28**:497–516.
26. **Garesse, R.** 1988. *Drosophila melanogaster* mitochondrial DNA: gene organization and evolutionary considerations. Genetics **118**:649–663.
27. **Garnier, J., D. J. Osguthorpe, and B. Robson.** 1978. Analysis of the accuracy and implications of a simple method for predicting the secondary structure of globular proteins. J. Mol. Biol. **120**:97–120.
28. **Giles-Gonzalez, M. A., G. S. Ditta, and D. R. Helinski.** 1991. A haemoprotein with kinase activity encoded by the oxygen sensor of *Rhizobium meliloti*. Nature (London) **350**:170–172.
29. **Guerlesquin, F. A., M. Bruschi, G. E. Bovier-Lapierre, J. J. Bonicel, and P. M. Couchoud.** 1983. Primary structure of the two (4Fe-4S) clusters ferredoxin from *Desulfovibrio desulfuricans* (strain Norway 4). Biochimie **65**:43–47.
30. **Hausinger, R. P., I. Moura, J. J. G. Moura, A. V. Xavier, M. H. Santos, J. Legall, and J. B. Howard.** 1982. Amino acid sequence of a 3F3:3S ferredoxin from the "archaebactrium" *Methanosarcina barkeri* (DSM800). J. Biol. Chem. **257**:14192–14197.
31. **Haydon, D. J., and J. R. Guest.** 1991. A new family of bacterial regulatory proteins. FEMS Microbiol. Lett. **79**:291–296.
32. **Huber, M., L. Garfinkel, C. Gitler, D. Mirelman, M. Revel, and S. Rozenblatt.** 1988. Nucleotide sequence analysis of an *Entamoeba histolytica* ferredoxin gene. Mol. Biochem. Parasitol.

31:27–34.
33. **Irwin, D. M., T. D. Kocher, and A. C. Wilson.** 1991. Evolution of the cytochrome b gene of mammals. J. Mol. Evol. **32:**128–144.
34. **Johnson, E. F., D. L. Walker, K. J. Griffin, J. E. Clark, R. T. Okita, A. S. Meurhoff, and B. S. Masters.** 1990. Cloning and expression of three rabbit kidney cDNAs encoding lauric acid omega-hydroxylases. Biochemistry **29:**873–879.
35. **Kahn, D., M. David, O. Domergue, M.-L. Daveran, J. Ghai, P. R. Hirsch, and J. Batut.** 1989. *Rhizobium meliloti fixGHI* sequence predicts involvement of a specific cation pump in symbiotic nitrogen fixation. J. Bacteriol. **171:**929–939.
36. **Keen, N. T., S. Tamaki, D. Kobayashi, and D. Trollinger.** 1988. Improved broad-host-range plasmids for DNA cloning in gram-negative bacteria. Gene **70:**191–197.
37. **Kendall, K. J., and S. N. Cohen.** 1988. Complete nucleotide sequence of the *Streptomyces lividans* plasmid pIJ101 and correlation of the sequence with genetic properties. J. Bacteriol. **170:**4634–4651.
38. **Klein, P., M. Kanehisa, and C. DeLisi.** 1985. The detection and classification of membrane-spanning proteins. Biochim. Biophys. Acta **815:**468–476.
39. **Kolaskar, A. S., and B. V. Reddy.** 1985. A method to locate protein coding sequences in DNA of prokaryotic systems. Nucleic Acids Res. **13:**185–194.
40. **Lee, J. K., and S. Kaplan.** 1992. *cis*-Acting regulatory elements involved in oxygen and light control of *puc* operon transcription in *Rhodobacter sphaeroides*. J. Bacteriol. **174:**1146–1157.
41. **Leuking, D. R., R. T. Fraley, and S. Kaplan.** 1978. Intracytoplasmic membrane synthesis in synchronous cell populations of *Rhodopseudomonas sphaeroides*. J. Biol. Chem. **253:**451–457.
42. **Lipman, D. J., and W. R. Pearson.** 1985. Rapid and sensitive protein similarity searches. Science **227:**1435–1441.
43. **Maniatis, T., E. F. Fritsch, and J. Sambrook.** 1982. Molecular cloning: a laboratory manual. Cold Spring Harbor Laboratory, Cold Spring Harbor, N.Y.
44. **Manoil, C., J. J. Mekalanos, and J. Beckwith.** 1990. Alkaline phosphatase fusions: sensors of subcellular location. J. Bacteriol. **172:**515–518.
45. **Masuda, T., H. Tatsumi, and E. Nakano.** 1989. Cloning and sequence analysis of cDNA for luciferase of a Japanese firefly *Luciolo cruciata*. Gene **77:**265–270.
46. **Matsubara, H., K. Inoue, T. Hase, H. Hiura, T. Kakuno, J. Yamashita, and T. Horio.** 1983. Structure of the extracellular ferredoxin from *Rhodospirillum rubrum* shows similarity to clostridial ferredoxins. J. Biochem. **93:**1385–1390.
47. **Messing, J.** 1979. A multipurpose cloning system based on single-stranded DNA bacteriophage M13. Recomb. DNA Tech. Bull. **2:**43–48.
48. **Minami, Y., S. Wakabayashi, K. Wada, H. Matsubara, L. Kerscher, and D. Oesterhelt.** 1985. Amino acid sequence of a ferredoxin from thermoacidophilic archaebacterium *Sulfolobus acidocaldarius*. Presence of an N^6-monomethyllysine and phyletic consideration of archaebacteria. J. Biochem. **97:**745–753.
49. **Moore, M. D., and S. Kaplan.** 1992. Identification of intrinsic high-level resistance to rare-earth oxides and oxyanions in members of the class *Proteiobacteria*: characterization of tellurite, selenite, and rhodium sesquioxide reduction in *Rhodobacter sphaeroides*. J. Bacteriol. **174:**1505–1514.
50. **Moore, M. D., and S. Kaplan.** Unpublished data.
51. **Mornet, E., J. Dupont, A. Vitek, and P. C. White.** 1989. Characterization of two genes encoding human steroid 11 beta-hydroxylase (P-450 (11) beta). J. Biol. Chem. **264:**20961–20967.
52. **Motojima, K., and S. Goto.** 1989. Cloning of rabbit uricase cDNA reveals a conserved carboxy-terminal tripeptide in three species. Biochim. Biophys. Acta **1008:**116–118.
53. **Neidle, E. L., and S. Kaplan.** Unpublished data.
54. **Okimoto, R., J. L. MacFarlane, D. O. Clary, and D. R. Wolstenholme.** 1990. Sequence submitted to EMBL and GenBank.
55. **Phillips, M. K., L. Hederstedt, S. Hasnain, L. Rutberg, and J. R. Guest.** 1987. Nucleotide sequence encoding the flavoprotein and iron-sulfur protein subunits of the *Bacillus subtilis* PY79 succinate dehydrogenase complex. J. Bacteriol. **169:**864–873.
56. **Prentki, P., and H. M. Krisch.** 1984. In vitro insertional mutagenesis with a selectable DNA fragment. Gene **29:**303–313.
57. **Rao, M. J. K., and P. Argos.** 1986. A conformational preference parameter to predict helices in integral membrane proteins. Biochim. Biophys. Acta **869:**197–214.
58. **Sanger, F., S. Nicklen, and A. R. Coulson.** 1977. Nucleotide sequencing with chain-terminating inhibitors. Proc. Natl. Acad. Sci. USA **74:**5463–5467.
59. **Sato, S., K. Nakazawa, K. Hon-Nami, and T. Oshima.** 1981. Purification, some properties and amino acid sequence of *Thermus aquaticus* HB8 ferredoxin. Biochim. Biophys. Acta **668:**277–289.
60. **Sciolo, J. R., and B. A. Zilinskas.** 1988. Cloning and characterization of a cDNA encoding the chloroplastic copper/zinc-superoxide dismutase from pea. Proc. Natl. Acad. Sci. USA **85:**7661–7665.
61. **Seki, Y., S. Seki, and M. Ishimoto.** 1989. The primary structure of *Clostridium perfringens* ferredoxin. J. Gen. Appl. Microbiol. **35:**167–172.
62. **Shine, J., and L. Dalgarno.** 1975. Determination of cistron specificity in bacterial ribosomes. Nature (London) **254:**34–38.
63. **Simon, R., U. Priefer, and A. Puhler.** 1983. A broad host range mobilization system for in vivo genetic engineering: transposon mutagenesis in Gram-negative bacteria. Bio/Technology **1:**37–45.
64. **Stephens, P. E., M. G. Darlison, H. M. Lewis, and J. R. Guest.** 1983. The pyruvate dehydrogenase complex of *Escherichia coli* K12. Nucleotide sequence encoding the pyruvate dehydrogenase component. Eur. J. Biochem. **133:**155–162.
65. **Suwanto, A., and S. Kaplan.** 1989. Physical and genetic mapping of the *Rhodobacter sphaeroides* 2.4.1 genome: genome size, fragment identification, and gene localization. J. Bacteriol. **171:**5840–5849.
66. **Suwanto, A., and S. Kaplan.** 1989. Physical and genetic mapping of the *Rhodobacter sphaeroides* 2.4.1 genome: presence of two unique circular chromosomes. J. Bacteriol. **171:**5850–5859.
67. **Suwanto, A., and S. Kaplan.** 1992. Chromosome transfer in *Rhodobacter sphaeroides*: Hfr formation and genetic evidence for two unique circular chromosomes. J. Bacteriol. **174:**1135–1145.
68. **Tai, T.-N., M. D. Moore, and S. Kaplan.** 1988. Cloning and characterization of the 5-aminolevulinate synthase gene(s) from *Rhodobacter sphaeroides*. Gene **70:**139–151.
69. **Van Neil, C. B.** 1944. The culture, general physiology, and classification of the non-sulfur purple and brown bacteria. Bacteriol. Rev. **8:**1–118.
70. **Varga, A. R., and S. Kaplan.** 1989. Construction, expression, and localization of a CycA::PhoA fusion protein in *Rhodobacter sphaeroides* and *Escherichia coli*. J. Bacteriol. **171:**5830–5839.
71. **Vieira, J., and J. Messing.** 1982. The pUC plasmids, and M13mp7-derived system for insertion mutagenesis and sequencing with synthetic universal primers. Gene **19:**259–268.
72. **Yanisch-Perron, C., J. Vieira, and J. Messing.** 1985. Improved M13 cloning vectors and host strains: nucleotide sequences of the M13mp18 and pUC19 vectors. Gene **33:**103–119.